Composites Part B 110 (2017) 361–367

Contents lists available at ScienceDirect

Composites Part B

journal homepage: www.elsevier.com/locate/compositesb

# Selective metallization on copper aluminate composite via laser direct structuring technology

Jong-uk Yang [a, b], Jin Han Cho [a], Myong Jae Yoo [b, *]

[a] Department of Chemical and Biological Engineering, Korea University, Seoul 136-701, Republic of Korea
[b] Electronic Materials & Device Research Center, Korea Electronics Technology Institute, Seongnam 463-816, Republic of Korea

ARTICLE INFO

*Article history:*
Received 26 July 2016
Received in revised form
7 October 2016
Accepted 15 November 2016
Available online 16 November 2016

*Keywords:*
Moulding compounds
Microstructure
Surface analysis
Injection moulding

ABSTRACT

This study focused on synthesizing copper aluminate and the compound's applicability to laser direct structuring technology. Since aluminum weighs less and costs less than chromium, this study investigated its potential as a substitute in copper chromate, the main additive of LDS materials. Copper aluminate was synthesized using a sol-gel method. The synthesized powder was then applied to two types of resin, polycarbonate (thermoplastic) and polyimide (thermosetting). After optimum processing at each laser parameter, the metal patterns are formed by electroless plating. Fabricated patterns were observed using optical microscopy. This study confirmed that copper aluminate can be used in LDS (Laser direct structuring) technology and that, furthermore, it supports the formation of conductive patterns with both thermoplastic and thermosetting resins.



## 1. Introduction

Due to the versatility of the injection molding and structured metallization process, mechanical and electrical functions can be directly integrated into a wide variety of molded interconnect devices (MIDs) [1]. The concept of molded circuit boards (MCBs) was introduced in the USA in 1983 and their industrial potential led to the development of MID technology in 1985 [2]. MCBs are made by combining the printing processes used to make classical printed circuit boards (PCBs) with injection molding [3]. MID fabrication is a multistep process. Most MID production starts with the injection molding of a thermoplastic part, and involves either single or two shot molding. In single shot molding, a single injection molding process of a thermoplastic material produces the MID, whereas in two shot molding, two successive injection molding processes are used, of which only the second layer is platable. The next steps of MID production are circuit structuring and selective metallization. Circuit structuring may be accomplished by various methods such as LDS (Laser Direct Structuring), LSS (Laser Subtractive Structuring) [4], two-shot molding [5], inkjet printing [6], hot stamping [7], and others [8].

Laser Direct Structuring (LDS) is a widely used and well known method of circuit structuring for MID fabrication, in which the circuit pattern is fabricated on molded thermoplastics through laser patterning and electroless plating. Fig. 1 shows the detailed steps of the LDS process. The molded part is subjected to laser activation, which activates the surface of the molded thermoplastic, allowing selective metallization to then form the conductive pattern [9] [10]. The advantages of this technology include great design flexibility, the possibility of making circuits on 3D surfaces and higher levels of product integration with improved quality and reduced costs. The technology also allows the production of ultra-fine structures with widths and gaps less than 100 μm [11].

Selective metallization takes place on composites doped with a LDS additive. The LDS additive is key to forming a conductive pattern. The LDS additive should initially be electrically non-conducting, thermally resistant to the injection molding process, well compatible with polymers, non-toxic and low cost for mass production. The preferred selective additive is a metal oxide or organic metal complex. The LDS additive is excited and separated into metal and organic residuals by laser irradiation [12]. This is called 'activation'. In electroless plating, the activated filler acts as a plating catalyst [13] [14]. Examples of activation fillers include $Al_2O_3$, $CeO_2$, ZnO, AlN, SIC, CuO and a Cu-Cr complex [15] [16]. When a laser is irradiated on the composite surface, the polymer matrix is removed (photo-chemical ablation) or evaporated [17], and the filler is exposed and activated. The activated filler donates

* Corresponding author. Department of Chemical and Biological Engineering, Korea University, Seoul 136-701, Republic of Korea.
*E-mail address:* jsayoo10@keti.re.kr (M.J. Yoo).

http://dx.doi.org/10.1016/j.compositesb.2016.11.041
1359-8368/

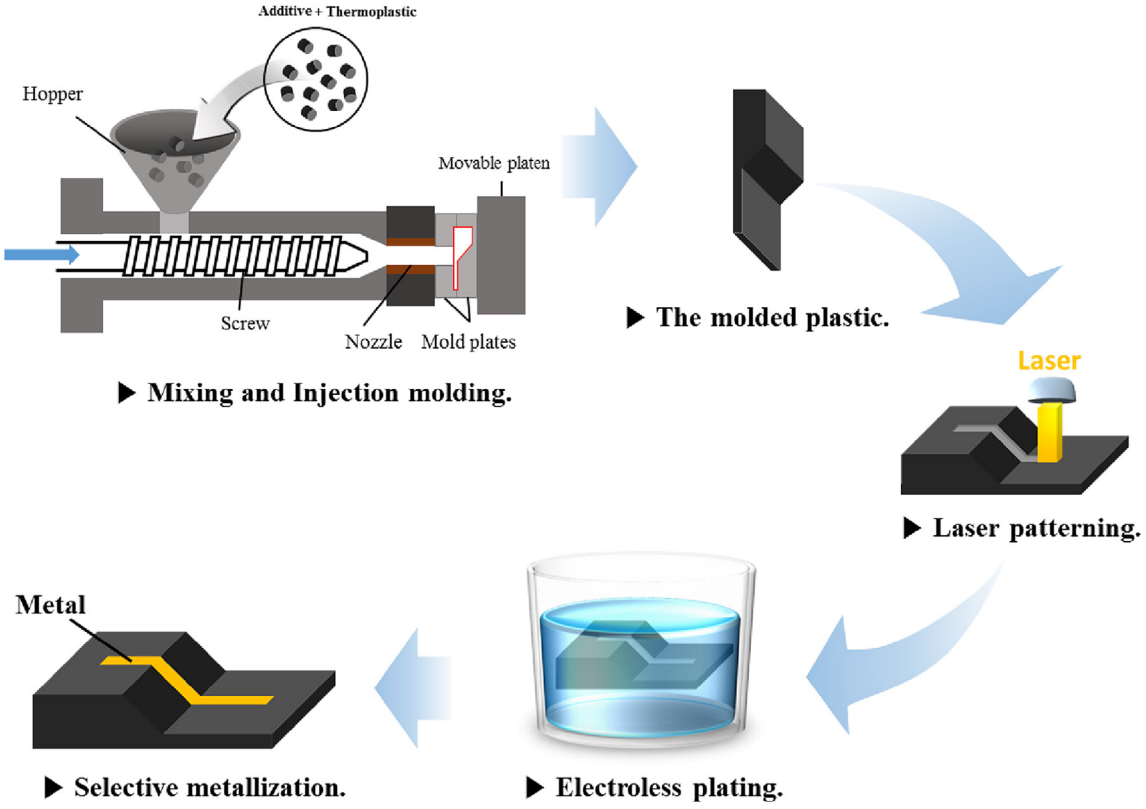


**Fig. 1.** Schematic of LDS process steps.

electrons in electroless plating [15] [18].

This study evaluated the characteristics of copper aluminate as the activation filler and investigated its potential in LDS technology applications. Copper aluminate was formed into nanoparticles using a sol-gel method [19] [20] [21] as nanoparticles are expected to be better able to form fine conductive patterns. Overall, this study confirmed that copper aluminate can form conductive patterns using LDS technology.

## 2. Experimental

### 2.1. Synthesis of copper aluminate

The copper aluminate was synthesized using a sol-gel method. Copper nitrate trihydrate ($Cu(NO_3)_2 \cdot 3H_2O$, 99–104%, Sigma-Aldrich) and aluminum nitrate nonahydrate ($Al(NO_3)_3 \cdot 9H_2O$, ≥98.0%, Sigma-Aldrich) was used as received. Citric acid ($HOC(COOH)(CH_2COOH)_2$, anhydrous, Sigma-Aldrich) was used as a complex agent. Firstly citric acid was dissolved in distilled water, followed by copper nitrate and aluminum nitrate. The molar ratio of citric acid to metal ions was fixed at 13:1 and that of copper nitrate to aluminum nitrate at 1:2. The solution was stirred until complete dissolution was achieved. The color of the solution was clear blue after 30 min. The solution was heated at 110 °C for 6 h to remove excess water. After excess water removal the solution became viscous indicating formation of the precursor had formed. The precursor was calcined at 600 °C for 5 h to remove organic matter, and, to finalize crystal structure formation, heated further at 900 °C

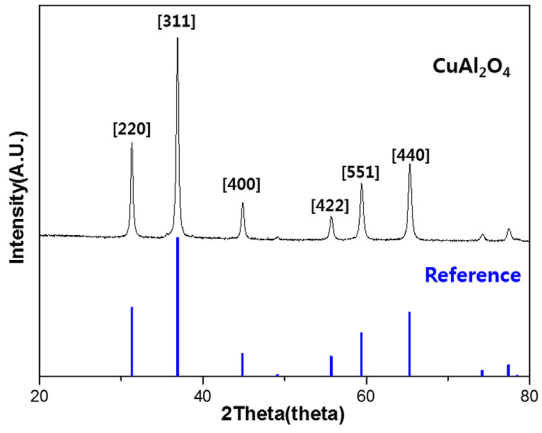


**Fig. 2.** XRD analysis of synthesized $CuAl_2O_4$ powder.

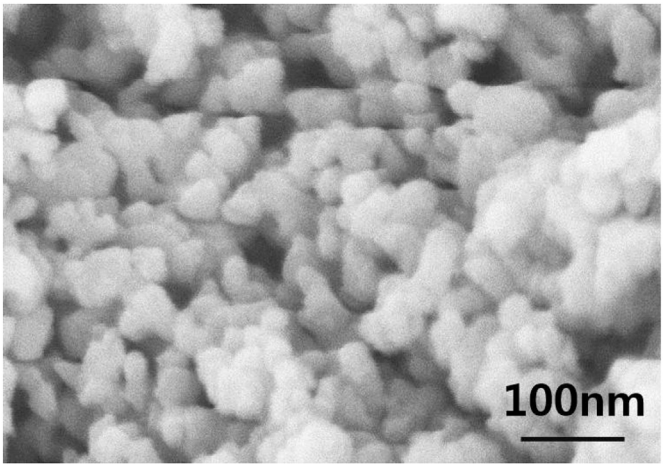


**Fig. 3.** High resolution scanning electron micrographs of synthesized $CuAl_2O_4$ powder.

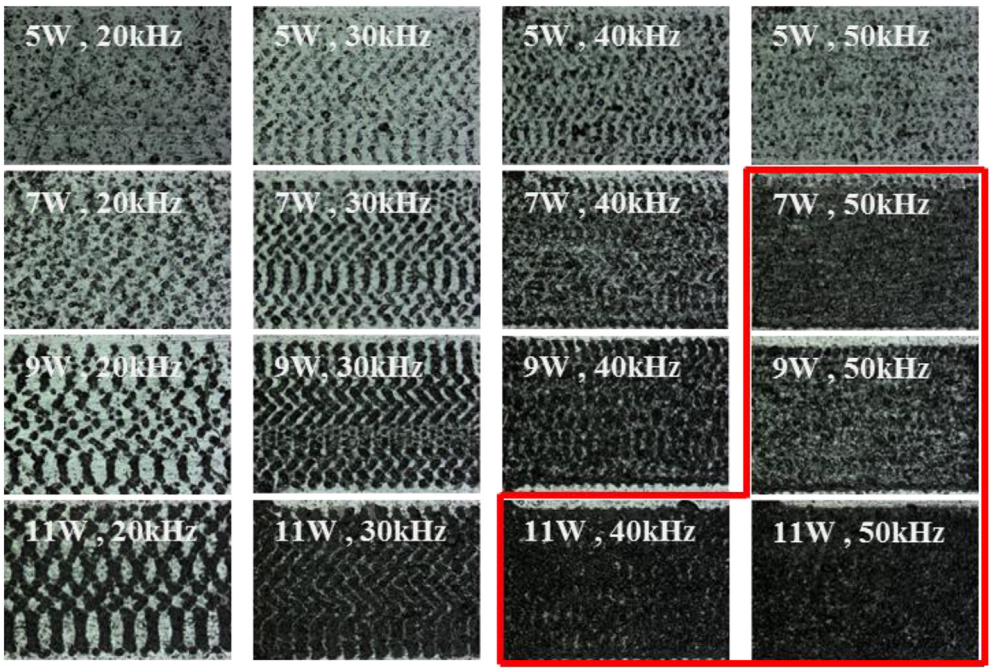


**Fig. 4.** Microscope image of surface pattern according to laser parameter. (Hatch width: 25 μm).

for 5 h in an air atmosphere.

### 2.2. Fabrication of copper aluminate composite

#### 2.2.1. Thermoplastic composite

Polycarbonate (PC) was selected as the thermoplastic resin. PC has the merits that it can be dissolved in solvents for mixing with copper aluminate and has a low oxidation rate when used in injection molding. The PC supplied by Cheil Industries Inc was first dissolved in Tetrahydrofuran (THF) to form a transparent 10% solid solution. Next, copper aluminate powder was added to the solution at 5 wt percent which was then sonicated for 5 min to enhance dispersion. The mixed solution was then dried at room temperature for 24 h. The dried mixture was finely crushed using an agate mortar and loaded into a mini injection molder (Bautek, Korea) for forming into a square bar shape. The injection molding process was done at 280 °C.

#### 2.2.2. Thermosetting composite

Polyimide (PI) was selected as the thermosetting resin, because of its superb chemical resistance, heat resistance, electric insulation, and flexibility [22] [23] [24]. The PI used was POLYZEN 150P supplied by Picomax. To ensure its uniform dispersion in spite of its high viscosity, ball milling was used. The solid loading of powder in PI solution was done at 2, 3 and 4 wt percent. The composite mixture was formed into film samples 70 μm thick using a tape casting process. The films were dried at 60 °C for 1 h, and finally cured at 220 °C for 1 h.

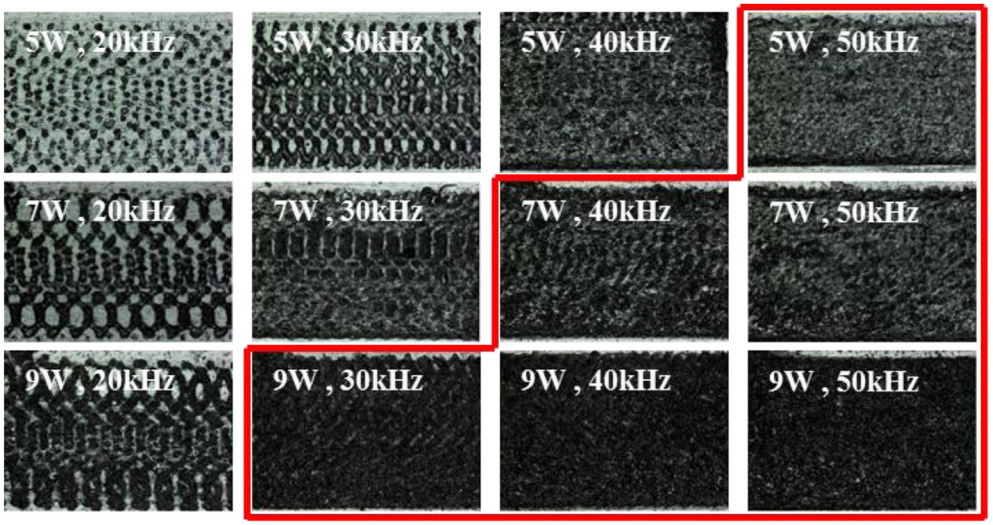


**Fig. 5.** Microscope image of surface pattern according to laser parameter. (Hatch width: 13 μm).

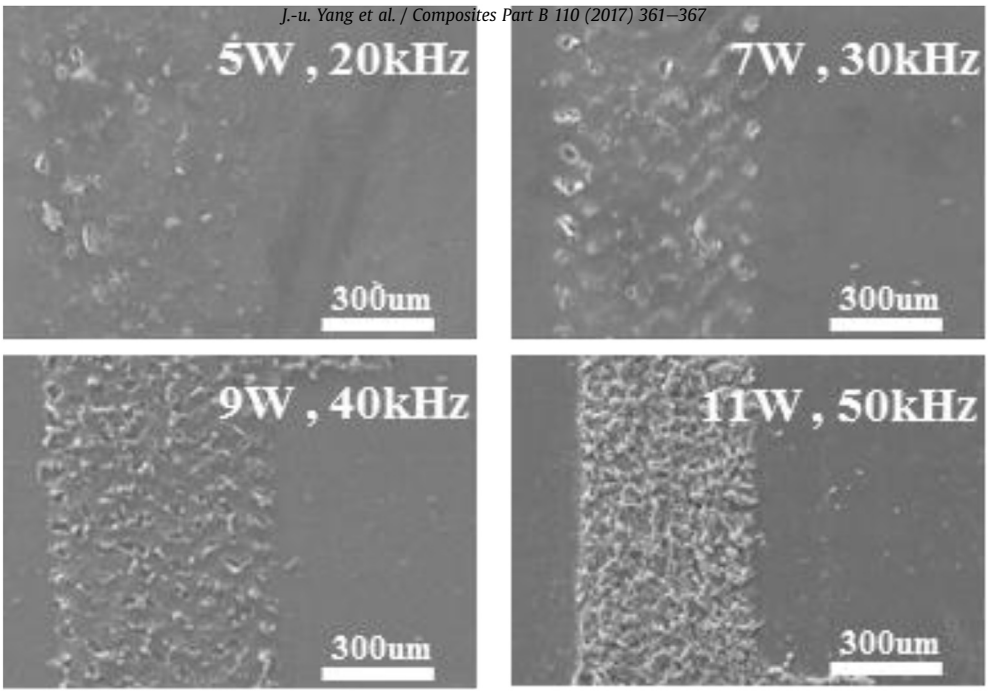


**Fig. 6.** SEM image of surface pattern of according to laser parameter. (Hatch width: 25 μm).

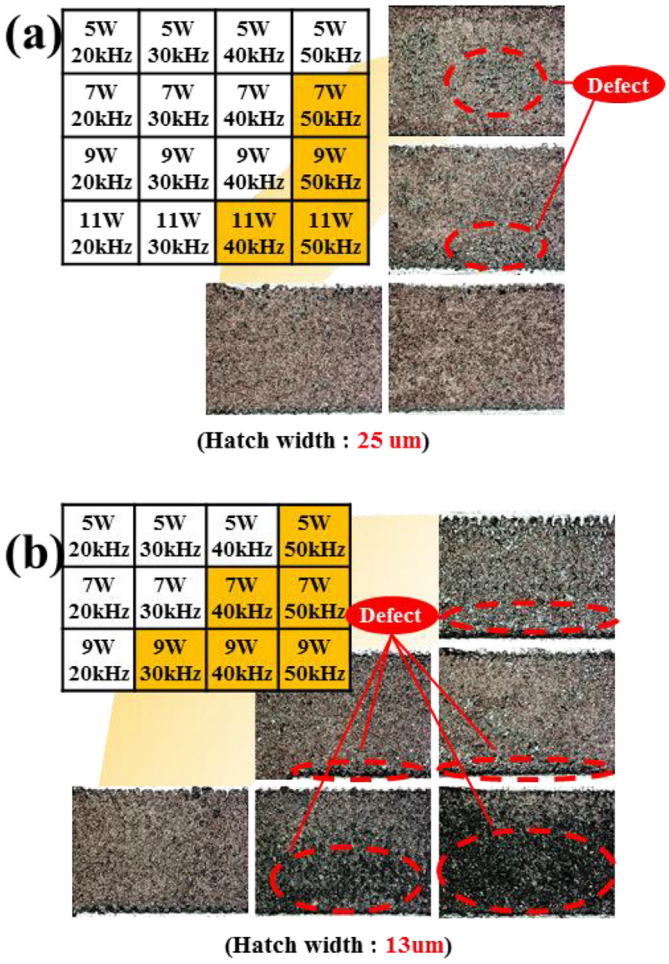


**Fig. 7.** Optical microscope image of surface of copper plated thermoplastic composite. (a) Hatch width: 25 μm; (b) Hatch width: 13 μm.

### 2.3. Characterization of copper aluminate

Structural characterization of the copper aluminate was performed using a RINT2000 vertical goniometer (Rigaku Co., Inc.) for 2θ values ranging from 20 to 80 ° using $CuK_\alpha$ radiation at $\lambda = 0.154$ nm. To determine the particle size and conduct an elemental analysis of the copper aluminate, HR-SEM images along with an energy dispersive X-ray analysis (EDX) were recorded using a S-4800 (Hitachi Co., Ltd.) high resolution scanning electron microscope. Thermogravimetric analysis (TGA) was carried out using a thermal gravimetric analysis instrument (STA-409, NETZSCH Co., Inc.) at a heating rate of 10 °C/min. The density of the synthesized copper aluminate powder was analyzed using the Gas Displacement Pycnometry System (AccuPyc 1330, Micromeritics Co., Inc.). The analysis was conducted under a pressure of 15 psig using helium gas, and the final density value was the average of 5 measurements.

### 2.4. Metallization

The laser patterning was done using an Nd:YAG pulse laser (1064 nm) with a maximum power of 20 W, repetition of 1000 kHz and spot size of 25 μm. The laser variables were power (5–11 W) and repetition (20–50 kHz). An electroless copper plating solution (ECP-90) was used as supplied from ECtech. The surface pattern formed on the copper aluminate composite by laser irradiation was observed using an optical microscope (VK-9710, Keyence Co., Ltd.).

## 3. Results and discussion

### 3.1. Characterization of copper aluminate

#### 3.1.1. X-ray diffraction analysis

The synthesized powder was measured by XRD for a crystalline analysis. As shown in Fig. 2, at 900 °C [220], [311], [400], [422], [511], and [440] crystal faces are present at 31.31 °, 36.91 °, 44.89 °, 55.76 °, 59.47 °, and 65.37 °, respectively, indicative of copper

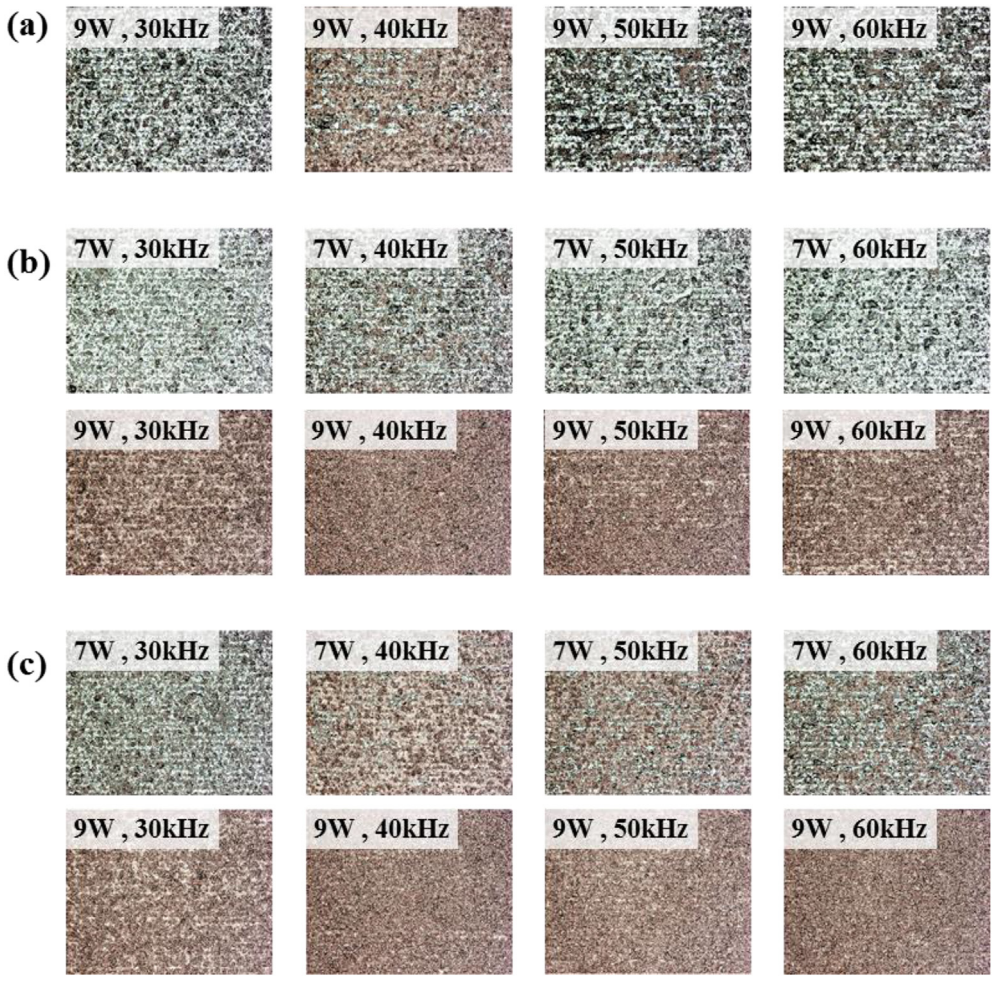


**Fig. 8.** Microscope image of electroless plating on surface according to laser parameter of copper aluminate composite using polyimide resin at (a) 2 wt%; (b) 3 wt%; (c) 4 wt%; filler loading.

aluminate (ICSD card no. 9557). The calculated lattice parameter was a = b = c = 8.07 Å from Bragg's law, showing that the crystal structure of the powder is cubic and spinel. Overall, the copper aluminate formed by the sol-gel method showed good crystallinity.

Crystal size ($D_c$) can be calculated from the XRD measurements using the Debey-Scherrer equation [25],

$$D_c = K\lambda/\beta\cos\theta$$

where β is the width of the observed diffraction line at its half-intensity maximum, K is the so-called shape factor, which usually takes a value of about 0.9, and k is the wavelength of the X-ray source used in the XRD analysis. The mean crystal size thereby calculated is 34.12 nm.

#### 3.1.2. Scanning electron microscope and density analysis

The morphology of the synthesized copper aluminate powder was investigated by scanning FE-SEM. Fig. 3 shows the images of the particles. The particle morphology was amorphous and uniform. The particle size was 30–50 nm, similar to the calculated crystal size.

The average density of the synthesized copper aluminate was 4.80 g/cm$^3$. The synthesized copper aluminate is 9.4% lighter than commercial copper chromite powder which has a density of 5.30 g/cm$^3$. Thus, copper aluminate powder is expected to form composites of lower density than copper chromite.

### 3.2. Optical microscope imaging of the composite

#### 3.2.1. Thermoplastic composite

The surface pattern of the thermoplastic copper aluminate composite created by laser irradiation was observed using an optical microscope. Fig. 4 shows the increasing uniformity of surface pattern as laser power and laser repetition increases at a hatch width of 25 μm. As shown in Fig. 5, similar results were obtained at a hatch width of 13 μm. These results indicate that to obtain the most uniform surface patterning at a hatch width of 25 μm, a laser power of 7–11 W with a repetition of 40–50 kHz is required. At a hatch width of 13 μm, uniform surface patterning formed at a laser power of 5–9 W and a repetition of 30–50 kHz. Fig. 6 shows SEM images of surface patterns formed under varying laser parameters (Hatch width: 25 μm).

After electroless plating with copper solution, metallization on the surface of the copper aluminate composite was observed by optical microscope. Fig. 7 shows the copper plated surface pattern, where defects were observed. In Fig. 7(a), the pattern was not plated due to low laser power and low repetition. Fig. 7(b) shows defects due to the smaller hatch width which induced overlapping and thus insufficient plating. As a result, the optimum laser variables for obtaining a uniform plating pattern was observed to

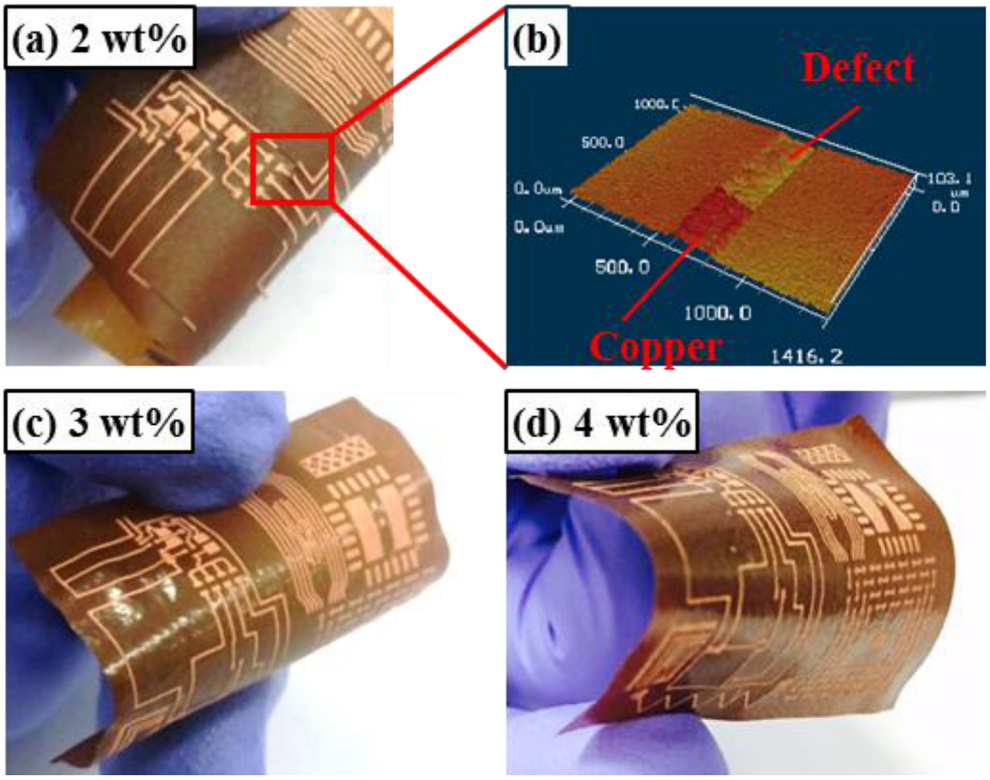


**Fig. 9.** Result of flexible circuit according to $CuAl_2O_4$ loading in polyimide at laser power of 9 W, repetition of 40 kHz (a) 2 wt%; (b) Defect on curved part; (c) 3 wt%; (d) 4 wt%.

be a power of 11 W, a repetition of 50 kHz and a hatch width of 25 μm.

### 3.2.2. *Thermosetting composite*

The thermosetting composite was fabricated into a film. It was necessary to find the minimum laser power, number of repetitions and copper aluminate powder content, because high laser power and repetition can puncture the film and high copper aluminate powder content can deteriorate the mechanical properties of film.

Fig. 8(a) shows surface plating according to laser variables at 2 wt percent copper aluminate. Overall the plating was not well formed. Fig. 8(b) shows surface plating according to laser variables at 3 wt percent copper aluminate. The surface plating was not well formed at a laser power of 7 W, but well formed at a laser power of 9 W. Uniform surface plating was achieved at a laser power of 9 W and a repetition of 40 kHz. Fig. 8(c) shows the surface plating according to laser variables at 4 wt percent copper aluminate. The surface plating was formed at a laser power of 7 W, unlike the results shown in Fig. 8(a) (b). Uniform surface plating was achieved at a laser power of 9 W.

Fig. 9 shows flexible circuit boards created with PI resin according to copper aluminate content. In Fig. 9(c) (d), the curved state caused no problem but Fig. 9(a) shows the occurrence of defects at the curved part. From this result, it is assumed that plating adhesion became weaker due to the low content of copper aluminate. Thus, the above results suggest that the minimum copper aluminate content for thermosetting composites is 3 wt percent.

## 4. Conclusions

This study focused on synthesizing copper aluminate and its applicability to make composite materials for laser direct structuring technology. Copper aluminate was synthesized via the sol-gel method. Characterization results show the achievement of a highly crystalline nature, smaller crystallite size and lower density than compared with copper chromite which is a commercial LDS additive. The copper aluminate was used to fabricate thermoplastic (PC) composite and thermoset (PI) composite. In thermoplastic (PC) composite, laser parameter for uniform surface patterning and plating was laser power of 11 W, repetition of 50 kHz, hatch width of 25 μm. In thermoset (PI) composite, optimum laser parameter for uniform surface patterning and plating was laser power of 9 W, repetition of 40 kHz, hatch width of 40 μm. This study confirmed that copper aluminate can be used for LDS technology. Detailed experiments acquired suitable laser patterning conditions for each thermoplastic and thermosetting composites fabricated with copper aluminate as LDS additive. Thus this study proposes new LDS additive material which is copper aluminate it has reduced density compared to commercial LDS additive. This effect is expected to contribute to lighter weight composite material for various electronic applications. Also for future study it is anticipated that by controlling the synthesized copper aluminate size fabrication of finer metal line patterns is possible which will enable more compact and miniaturized circuit formation.

## Acknowledgements

This work was supported by a grant from the Knowledge Economy Technology Innovation (Grant 10063453) for Global Expertise Development, Republic of Korea.

## References

[1] Franke J, Jürgenhake C, Schierbaum T, Fischer C, Dumitrescu R. Three-dimensional molded interconnect devices (3D-MID). 2014. http://dx.doi.org/10.3139/9781569905524.
[2] Zhuo Y, Du XL, Zhu JQ. Three-dimensional automatic routing for the design of

moulded interconnect devices. Int J Comput Integr Manuf 2011;24:302–11. http://dx.doi.org/10.1080/0951192x.2011.554871.
[3] Mapleston P. 3-D interconnects offer sizeable market opportunity. Mod Plast 1999;76:38.
[4] Application EP. European patent application, 1; 2012. p. 1–58.
[5] Islam A, Hansen HN, Tang PT, Sun J. Process chains for the manufacturing of molded interconnect devices. Int J Adv Manuf Technol 2009;42:831–41. http://dx.doi.org/10.1007/s00170-008-1660-9.
[6] Paulsen JA, Renn M, Christenson K, Plourde R. Printing conformal electronics on 3D structures with aerosol jet technology. FIIW 2012-2012 Futur Instrum Int Work Proc 2012:47–50. http://dx.doi.org/10.1109/FIIW.2012.6378343.
[7] Khuntontong P, Blaser T, Schomburg WK. Fabrication of molded interconnection devices by ultrasonic hot embossing on thin polymer films. IEEE Trans Electron Packag Manuf 2009;32:152–6. http://dx.doi.org/10.1109/TEPM.2009.2020742.
[8] Unnikrishnan D. And antennas potentiel de la technologie MID pour les composants passifs et des antennes. 2015.
[9] LPKF LDS, http://www.lpkf.fr/_mediafiles/1797-lpkf-ldsprocess.pdf.
[10] Kordass T, Franke J. Galvanic plating for 3D – MID applications n.d.:491–495.
[11] Schlüter R, Rösener B, Kickelhain J, Naundorf G. Completely additive laser-based process for the production of 3D MIDs–the LPKF LDS process. 5th int congr molded interconnect devices. Erlangen 2002.
[12] Huske M, Kickelhain J, Muller J, Eber G. Laser supported activation and additive metallization of thermoplastics for 3D-MIDs. Proc 3rd LANE 2001.
[13] Yung KC, Chen C, Lee CP. Laser induced activation of circuit lines and via-holes on AlN for electroless metal plating. Appl Surf Sci 2011;257:6601–6. http://dx.doi.org/10.1016/j.apsusc.2011.02.085.
[14] Cao S, Pedraza aJ, Allard LF. Laser-induced microstructural changes and decomposition of aluminum nitride. J Mater Res 1995;10:54–62. http://dx.doi.org/10.1557/JMR.1995.0054.
[15] Shafeev GA. Laser activation and metallisation of insulators. Quantum Electron 1997;27:1104–10. http://dx.doi.org/10.1070/Qe1997v027n12abeh001106.
[16] Liu T, Zhao M, Wang B, Wang M. Analysis of chemical property for CuCr complex surface by laser irradiation with different wavelength and laser mode. Opt Laser Technol 2012;44:1762–8. http://dx.doi.org/10.1016/j.optlastec.2011.12.003.
[17] Heininger N, John W, Boßler H. Fertigung von MID Bauteilen vom rapid prototyping bis zur Serie mit innovativer LDS-Technologie. 2004. p. 1–20.
[18] DeSilva MJ, Pedraza AJ, Lowndes DH. Electroless copper films deposited onto laser-activated aluminum nitride and alumina. J Mater Res 1993;9:1019–27. http://dx.doi.org/10.1557/JMR.1994.1019.
[19] Salavati-Niasari M, Davar F, Farhadi M. Synthesis and characterization of spinel-type $CuAl_2O_4$ nanocrystalline by modified sol-gel method. J Sol-Gel Sci Technol 2009;51:48–52. http://dx.doi.org/10.1007/s10971-009-1940-3.
[20] Kumar RT, Suresh P, Selvam NCS, Kennedy LJ, Vijaya JJ. Comparative study of nano copper aluminate spinel prepared by sol-gel and modified sol-gel techniques: structural, electrical, optical and catalytic studies. J Alloys Compd 2012;522:39–45. http://dx.doi.org/10.1016/j.jallcom.2012.01.064.
[21] Ragupathi C, Vijaya JJ, Kennedy LJ, Bououdina M. Nanostructured copper aluminate spinels: synthesis, structural, optical, magnetic, and catalytic properties. Mater Sci Semicond Process 2014;24:146–56. http://dx.doi.org/10.1016/j.mssp.2014.03.026.
[22] Jin X, Deng Y, Cai W, Lau W, Hui D, Yan H, et al. Material design and process development of electrostatically patterning silver capsuled composite particle for preparing conductive tracks on flexible substrate. Compos Part B 2016;105:111–5. http://dx.doi.org/10.1016/j.compositesb.2016.07.010.
[23] Fajstavr D, Alena Ř, Slepi P, Václav Š. Annealing of gold nanolayers sputtered on polyimide and polyetheretherketone, vol. 616; 2016. p. 188–96. http://dx.doi.org/10.1016/j.tsf.2016.08.025.
[24] Xu S, Zhang Y, Cho J, Lee J, Huang X, Jia L, et al. Stretchable batteries with self-similar serpentine interconnects and integrated wireless recharging systems. Nat Commun 2013;4:1543–8. http://dx.doi.org/10.1038/ncomms2553.
[25] Boubekri R, Beji Z, Elkabous K, Herbst F, Viau G, Ammar S, et al. Annealing effects on Zn (Co) O: from para-to ferromagnetic behavior. Chem Mater 2009;21:843–55.